Power dissipation analysis in tapping-mode atomic force microscopy

M. Balantekin* and A. Atalar
Bilkent University, Electrical Engineering Department, Bilkent, TR-06800, Ankara, Turkey
(Received 6 February 2003; published 27 May 2003)

In a tapping-mode atomic force microscope, a power is dissipated in the sample during the imaging process. While the vibrating tip taps on the sample surface, some part of its energy is coupled to the sample. Too much dissipated power may mean the damage of the sample or the tip. The amount of power dissipation is related to the mechanical properties of a sample such as viscosity and elasticity. In this paper, we first formulate the steady-state tip-sample interaction force by a simple analytical expression, and then we derive the expressions for average and maximum power dissipated in the sample by means of sample parameters. Furthermore, for a given sample elastic properties we can determine approximately the sample damping constant by measuring the average power dissipation. Simulation results are in close agreement with our analytical approach.

DOI: 10.1103/PhysRevB.67.193404 PACS number(s): 68.37.Ps, 62.25.+g

Tapping-mode force microscopy is utilized for surface imaging at very low lateral forces. The cantilever taps on the sample surface giving rise to the interaction force. This force has two parts: One is the attractive van der Waals (vdW) forces and second is the repulsive Hertzian contact force. These forces pull the sample surface up and down meaning that some part of the cantilever energy is dissipated in the sample where the sample can be modeled with a dashpot and a spring (see Fig. 1). If the dissipated power is high enough it can break the bonds of the surface atoms. Therefore, for nondestructive imaging the power dissipation is an important factor to consider. There are several studies[1–3] which relate the dissipated power to the phase of the cantilever. In this Brief Report we follow a completely different approach: First we obtain an analytical expression of tip-sample interaction force for a given steady-state tip oscillation amplitude, and then we give the power dissipation in terms of sample parameters. We assume that the higher harmonics of the cantilever oscillation is negligible, which is usually the case for high-Q systems, and hence the point-mass model describes the tapping-mode AFM suitably.[4] In this way we can easily find the dissipated power and compare it with our simulation[5] result. Moreover, we can find the sample damping constant by measuring the average power dissipation.

The tip-sample interaction is highly nonlinear and cannot be solved analytically without doing crude approximations. The simulations are quite useful to interpret experimental observations.[5,6] However, the simulations does not give an insight on the effect of overall system parameters. In order to gain further insight, we first need to approximate the nonlinear interaction force analytically at a given steady-state tip oscillation amplitude. In a tapping mode, there exist two stable oscillation states.[7] For the high amplitude solution, the tip-sample interaction force f_{TS} has both attractive and repulsive parts as shown in Fig. 2. The repulsive force for $0 \leqslant |t| < T_1$ can be approximated by a cosine. A linear approximation is utilized for the attractive force for $T_1 \leqslant |t| \leqslant T_2$. We assume that the force is even symmetric around $t=0$. An analytic expression for the interaction force can be written as

$$f_{\mathrm{TS}}(t)=\begin{cases} \dfrac{F_p-F_m}{1-\cos(2\pi/\alpha)}\cos\left(\dfrac{2\pi}{\alpha T_1}t\right)+\dfrac{F_m-F_p\cos(2\pi/\alpha)}{1-\cos(2\pi/\alpha)} & \text{for } 0\leqslant|t|<T_1 \\ \dfrac{F_m}{T_1-T_2}t+\dfrac{F_mT_2}{T_2-T_1} & \text{for } T_1\leqslant|t|\leqslant T_2 \\ 0 & \text{for } T_2<|t|\leqslant T/2. \end{cases} \tag{1}$$

In this parametric expression, F_p and F_m are the maximum repulsive and attractive forces exerted on the sample, respectively. T is the period of oscillation. α is a fit constant that defines the period of the cosine and its optimum value is different for different oscillation amplitudes. The results for different α values are very close to each other and hence for simplicity we choose $\alpha=4$. In the steady-state conditions, the periodic interaction force can be represented with a Fourier series[8]

$$f_{\mathrm{TS}}(t)=a_0+\sum_{n=1}^{\infty}a_n\cos(nwt), \tag{2}$$

where $w=2\pi/T$ is the oscillation frequency and the series coefficients are

$$a_0=\frac{2}{T}\int_0^{T/2}f_{\mathrm{TS}}(t)\,dt, \tag{3}$$

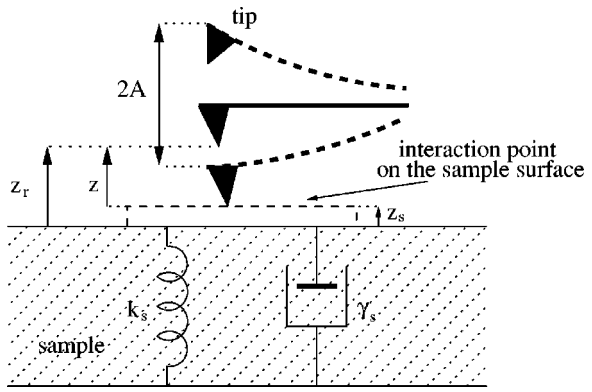

FIG. 1. The probing tip contains information about sample parameters. Mechanical behavior of the sample is modeled with a dashpot and a spring. Positions are referred with respect to the rest position of the sample surface.

$$a_n=\frac{4}{T}\int_0^{T/2} f_{\mathrm{TS}}(t)\cos(nwt)dt. \tag{4}$$

Using Eq. (1) in Eq. (4) we can find

$$a_n=\frac{8T_1(F_p-F_m)\cos(nwT_1)}{\pi T\left[1-\left(\frac{4nT_1}{T}\right)^2\right]} + \frac{TF_m[\cos(nwT_2)-\cos(nwT_1)]}{(T_1-T_2)(\pi n)^2}. \tag{5}$$

Referring to Fig. 1 the time T_2 can be found from geometric considerations as

$$T_2=\frac{T}{2}-\frac{T}{2\pi}\cos^{-1}\left(\frac{z_i-z_r-z_p e^{-k_s(T-T_2)/\gamma_s}}{A}\right), \tag{6}$$

here z_r is the rest position of the tip, A is the tip oscillation amplitude, k_s and γ_s are the sample spring constant and damping constant, respectively. z_i is the interaction distance where the attractive force is large enough to pull up the sample surface. z_p is the sample displacement due to maximum repulsive force exerted on the sample during previous cycle. Note that T_2 depends on itself, therefore the final value of T_2 is found by iteration.

Attractive part of the interaction force as a function of tip-sample distance z is given by[9]

$$F_{\mathrm{att}}(z)=\frac{HR}{6\sigma^2}\left[-\left(\frac{\sigma}{z}\right)^2+\frac{1}{30}\left(\frac{\sigma}{z}\right)^8\right] \quad \text{for } z>z_0=\frac{\sigma}{\sqrt[6]{30}}, \tag{7}$$

where H is the Hamaker constant, R is the tip radius, and σ is the interatomic distance. The effect of this force is negligible for tip to sample distances larger than 20σ. Therefore we choose $z_i=20\sigma$. The maximum attractive force F_m is found by setting the derivative of F_{att} equal to zero:

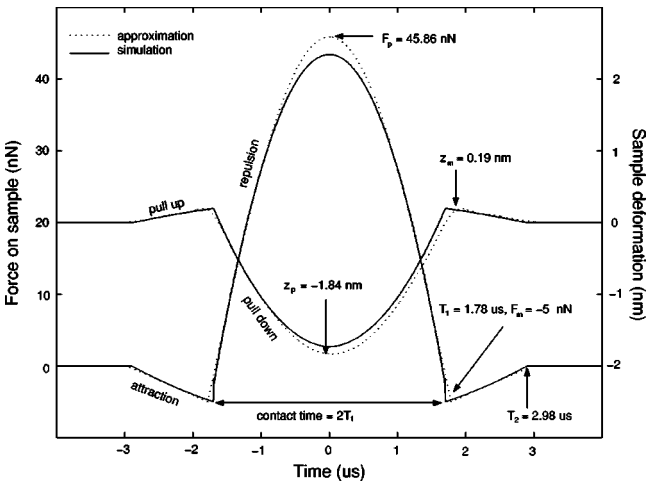

FIG. 2. A representative simulated and approximated forces and sample deformation in a fraction of one oscillation cycle. $A/A_0=0.8$, $\gamma_s=10^{-6}$ kg/s, $k_s=20$ N/m.

$$F_m=F_{\mathrm{att}}\left(z_a=z\Big|_{\partial F_{\mathrm{att}}/\partial z=0}=\frac{\sigma}{\sqrt[6]{15/2}}\right)=-0.245\frac{HR}{\sigma^2}. \tag{8}$$

The time T_1 when the attractive force reaches its maximum value is given by

$$T_1=\frac{T}{2}-\frac{T}{2\pi}\cos^{-1}\left(\frac{z_a-z_m-z_r}{A}\right), \tag{9}$$

where the sample deformation in the presence of F_m is

$$z_m=\frac{F_m}{k_s(T_2-T_1)}[(T_2-T_1)-(\gamma_s/k_s)(1-e^{-k_s(T_2-T_1)/\gamma_s})] - z_p e^{-k_s(T-T_1)/\gamma_s}. \tag{10}$$

Repulsive part of the interaction force is given by[9]

$$F_{\mathrm{rep}}(z)=\frac{8\sqrt{2R}}{3}E_r(z_0-z)^{3/2} \text{for } z\leqslant z_0, \tag{11}$$

$$\frac{1}{E_r}=\frac{1-v_t^2}{E_t}+\frac{1-v_s^2}{E_s}, \tag{12}$$

where E_r is the reduced elastic modulus of tip and sample. E_t, E_s and v_t, v_s are the Young's moduli and Poisson's ratios of the tip and sample, respectively. Using phasor analysis,[5] the fundamental component of f_{TS} can be found as

$$a_1=\frac{k_t}{Q_t}(A_0^2+A^2-2A_0A\sin\phi)^{1/2}\left[\left(1-\frac{w^2}{w_0^2}\right)^2Q_t^2+\frac{w^2}{w_0^2}\right]^{1/2}, \tag{13}$$

where A_0 is the free tip oscillation amplitude, w_0 is the resonance frequency, A and ϕ are the steady-state tip oscillation amplitude and phase, and k_t and Q_t are the spring constant and quality factor of the cantilever. If the cantilever is driven at its resonance frequency and assuming even symmetric interaction forces, Eq. (13) reduces to

$$a_1 = \frac{k_t}{Q_t}(A_0^2 - A^2)^{1/2}. \tag{14}$$

F_p and z_r must satisfy the following equations simultaneously:

$$a_1 = \frac{8T_1(F_p - F_m)\cos(wT_1)}{\pi T\left[1 - \left(\frac{4T_1}{T}\right)^2\right]} + \frac{TF_m[\cos(wT_2) - \cos(wT_1)]}{\pi^2(T_1 - T_2)}, \tag{15}$$

$$F_p = \frac{8\sqrt{2R}}{3}E_r(z_0 - z_r + A - z_p)^{3/2}, \tag{16}$$

where the sample displacement when F_p is exerted on the sample is

$$z_p = \frac{F_p}{k_s} + \left(z_m - \frac{F_m}{k_s}\right)e^{-k_s T_1/\gamma_s} + \frac{\gamma_s(F_m - F_p)(1 - e^{-k_s T_1/\gamma_s})}{k_s^2 T_1}. \tag{17}$$

The displacement of the sample surface due to f_{TS} is governed by the following differential equation

$$\gamma_s \frac{dz_s(t)}{dt} + k_s z_s(t) = f_{\mathrm{TS}}(t), \tag{18}$$

using superposition, we can add the displacements due to different frequencies to get the total displacement

$$z_s(t) = \frac{a_0}{k_s} + \sum_{n=1}^{\infty} \frac{a_n}{\sqrt{k_s^2 + (nw\gamma_s)^2}}\cos\left[nwt - \tan^{-1}\left(\frac{nw\gamma_s}{k_s}\right)\right]. \tag{19}$$

The instantaneous power dissipated in the sample is given by

$$p(t) = f_{\mathrm{TS}}(t)\frac{dz_s(t)}{dt}. \tag{20}$$

If we integrate $p(t)$ over one cycle and divide by the period, we get the average power. Hence we obtain our final result

$$P_{\mathrm{avg}} = \sum_{n=1}^{\infty} \frac{a_n^2}{2\sqrt{\gamma_s^2 + (k_s/nw)^2}}\sin\left[\tan^{-1}\left(\frac{nw\gamma_s}{k_s}\right)\right]. \tag{21}$$

Figure 3 shows the average power dissipated in one cycle for $A/A_0 = 0.8$. The parameters used in calculations are chosen to be $A_0 = 100$ nm, $f = w/2\pi = 20$ kHz, $k_t = 16$ N/m, $Q_t = 250$, $E_t = 90$ GPa, $E_s = 2$ GPa, $v_t = v_s = 0.2$, $H = 80$ zJ, $R = 10$ nm, and $\sigma = 2$ Å. Taking the first 100 terms in Eq. (21) provides less than 1% error. It is seen that the calculated and the simulated power values are in agreement.

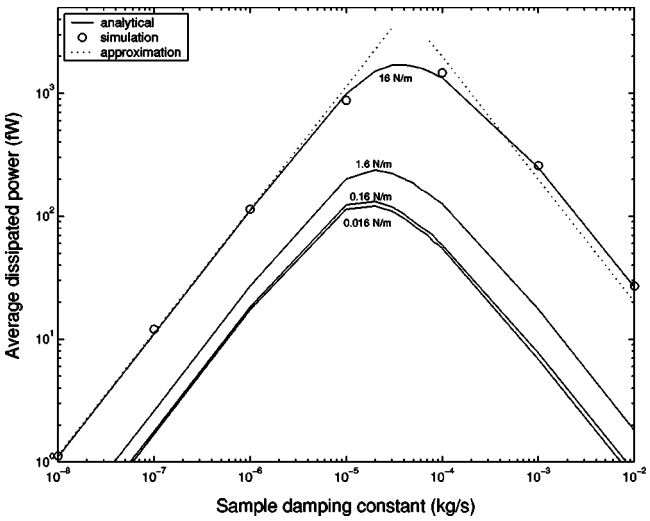

FIG. 3. Average dissipated power versus sample damping constant for various k_t values.

Now, we consider two asymptotic cases: For very low damping constants ($\gamma_s/k_s \ll T_1$), Eq. (21) can be approximated as

$$P_{\mathrm{avg}} \approx \sum_n \left(\frac{a_n nw}{k_s}\right)^2 \frac{\gamma_s}{2}. \tag{22}$$

Rearranging Eq. (22) we get

$$\gamma_s = \frac{2P_{\mathrm{avg}}}{\sum_n \left(\frac{a_n nw}{k_s}\right)^2}. \tag{23}$$

The sample spring constant k_s is proportional to the Young's modulus of the sample[10] and for this analysis it is taken to be $E_s R$. For very high damping constants ($\gamma_s/k_s \gg T$), the average power dissipation is given by

$$P_{\mathrm{avg}} \approx \frac{\sum_n a_n^2}{2\gamma_s}. \tag{24}$$

Rearranging Eq. (24) we get

$$\gamma_s = \frac{\sum_n a_n^2}{2P_{\mathrm{avg}}}. \tag{25}$$

The average power dissipation is also related to the tip oscillation amplitude A and phase ϕ by the following equation:[1–3]

$$P_{\mathrm{avg}} = \frac{k_t w}{2Q_t}[A_0 A \sin\phi - (w/w_0)A^2]. \tag{26}$$

Hence, we are able to estimate the sample damping constants by measuring the average power dissipation. As can be seen from Eqs. (17) and (10) z_p and z_m are zero for high damping constants, and they are equal to F_p/k_s and F_m/k_s for low

TABLE I. Actual and estimated γ_s values.

Multiplying factor	Actual γ_s	Estimated γ_s	Estimated γ_s with 10% error included in H	10% error included in R	10% error included in P_{avg}	50% error included in H	50% error included in R	50% error included in P_{avg}
10^{-8}	1.00	1.04	1.04 ± 0.02	1.04 ± 0.02	1.04 ± 0.11	1.05 ± 0.12	1.06 ± 0.13	1.04 ± 0.53
10^{-7}	1.00	1.04	1.04 ± 0.02	1.04 ± 0.02	1.04 ± 0.11	1.05 ± 0.12	1.06 ± 0.13	1.04 ± 0.53
10^{-6}	1.00	1.01	1.01 ± 0.02	1.01 ± 0.02	1.01 ± 0.10	1.01 ± 0.12	1.02 ± 0.13	1.01 ± 0.50
10^{-5}	1.00	0.77	0.77 ± 0.02	0.77 ± 0.02	0.77 ± 0.08	0.78 ± 0.09	0.78 ± 0.10	0.78 ± 0.39
10^{-4}	1.00	1.36	1.36 ± 0.03	1.34 ± 0.05	1.37 ± 0.14	1.36 ± 0.10	1.32 ± 0.23	1.81 ± 0.90
10^{-3}	1.00	0.78	0.78 ± 0.02	0.79 ± 0.03	0.78 ± 0.08	0.78 ± 0.06	0.78 ± 0.14	1.06 ± 0.54
10^{-2}	1.00	0.76	0.76 ± 0.04	0.77 ± 0.03	0.76 ± 0.08	0.76 ± 0.06	0.76 ± 0.13	1.00 ± 0.50

damping constants, respectively. Equations (22) and (24) are also plotted in Fig. 3. The approximation is valid for either low or high damping constants, it deviates from the exact result for medium γ_s values.

The procedure to find γ_s for a sample with known elasticity can be stated as follows. First, the interaction force parameters are found using Eqs. (6)–(17). Using Eq. (5) a_n values are calculated. The average power given by Eq. (26) is determined. Finally, γ_s values are found using Eqs. (23) or (25). A MATLAB code that does these calculations is available for download.[11]

To calculate the error bounds, we made several simulations. Table I summarizes the results. The Hamaker constant H depends on tip-sample system geometry, and the tip radius R can roughly be estimated. Therefore we include the errors coming from these constants into our analysis. It is seen that the phase measurement error in P_{avg} is dominant. Also, it is interesting to see that adding a 50% uncertainty to H or R does not significantly alter the results.

To find the maximum power dissipation, we equate $d^2z_s(t)/dt^2$ to zero and get

$$t=\frac{1}{nw}\left[\pi/2+\tan^{-1}\left(\frac{nw\gamma_s}{k_s}\right)\right]. \tag{27}$$

Substituting Eq. (27) into Eq. (20) we get

$$P_{\max}=\sum_n \frac{a_n}{\sqrt{\gamma_s^2+(k_s/nw)^2}}\sum_n a_n\sin\left[\tan^{-1}\left(\frac{nw\gamma_s}{k_s}\right)\right]. \tag{28}$$

Although the average power dissipation is in femtowatt levels, we have to consider the peak power dissipated in the sample. It is found that the peak instantaneous power can be more than 100 times the average power.

In summary, we formulated the average and maximum power dissipation in terms of the sample parameters. This analytical approach also gives a physical meaning to the phase ϕ of the cantilever [see Eqs. (21) and (26)]. It is clear that ϕ is a complicated function of the tip and the sample parameters as well as the oscillation amplitude. In addition, we are able to find many important quantities such as the contact time, the sample deformation, and the maximum forces exerted on the sample analytically. We also see from Fig. 3 that softening the lever more and more does not significantly reduce the power dissipation which is not seen directly from Eq. (26).

*Email address: mujdat@ee.bilkent.edu.tr

[1] J. Tamayo and R. Garcia, Appl. Phys. Lett. **73**, 2926 (1988).
[2] J. P. Cleveland, B. Anczykowski, A. E. Schmid, and V. B. Elings, Appl. Phys. Lett. **72**, 2613 (1998).
[3] B. Anczykowski, B. Gotsmann, H. Fuchs, J. P. Cleveland, and V. B. Elings, Appl. Surf. Sci. **140**, 376 (1999).
[4] T. R. Rodriguez and R. Garcia, Appl. Phys. Lett. **80**, 1646 (2002).
[5] M. Balantekin and A. Atalar, Appl. Surf. Sci. **205**, 86 (2003).
[6] O. Sahin and A. Atalar, Appl. Phys. Lett. **78**, 2973 (2001).
[7] R. Garcia and A. SanPaulo, Phys. Rev. B **61**, R13 381 (2000).
[8] R. W. Stark and W. M. Heckl, Surf. Sci. **457**, 219 (2000).
[9] M. Hoummady, E. Rochat, and E. Farnault, Appl. Phys. A: Mater. Sci. Process. **66**, S935 (1998).
[10] R. G. Winkler, J. P. Spatz, S. Sheiko, M. Möller, P. Reineker, and O. Marti, Phys. Rev. B **54**, 8908 (1996).
[11] URL: www.ee.bilkent.edu.tr/~mujdat